https://doi.org/10.26651/allelo.j/2020-51-1-1298 0971-4693/94 Euro 20.00
Allelopathy Journal 51 (2):165-176 (November, 2020) I*nternational Allelopathy Foundation* 2020
Tables: 4, Figs : 4

Allelopathic effects of phenolic acids on germination of watermelon (*Citrullus lanatus* Thunb): Dose-effect relationship and quantitative structure-activity relationship

Min Li[*], Lu Ma, Yuan Song, Xingfu Yan, Qian Lei and Xiu Zhang[1]

College of Biological Science and Engineering, North Minzu University,
Yinchuan 750021, Ningxia, China
E-mail: bkdlimin@126.com

(Received in revised form: July 29, 2020)

ABSTRACT

To determine the allelopathic potential of phenolic acids on watermelon (*Citrullus lanatus* Thunb), we studied the inhibitory activities of 21 phenolic acids on watermelon seeds germination. The quantitative structure-activity relationship (QSAR) method using the comparative molecular field analysis and comparative molecular similarity index analysis was used to elucidate the relationships between the inhibitory activities and structural characteristics. The results showed that half-maximal inhibitory concentrations (IC_{50}) were in ~μg/mL. The QSAR calculations suggested that the allelopathic inhibitory activities were increased when substituents had large moieties at 1/2/3/4-positions, negative charge at 1/3-position, a H-bond donor at 4-position and a H-bond acceptor at 2-position.

Keywords: Allelopathy, *Citrullus lanatus*, germination, phenolic acids, QSAR, structure-activity relationship, watermelon

INTRODUCTION

Phenolic acids (a big group of secondary metabolites), are found throughout the plant kingdom. Benzoic acid, syringic acid, salicylic acid, *p*-hydroxybenzoic acid, ferulic acid, gallic acid, vanillic acid, caffeic acid, *p*-coumaric acid and cinnamic acid have been identified by HPLC in extracts of plant parts and root exudates (5,17). Potential biological functions of phenolic acids viz., antioxidant (6), anticarcinogenic, antimicrobial (16) and allelopathic activities, are currently hot research topic. Phenolic acids enter the environment through root exudation, residue decomposition, pollen transfer, rain leachates etc., however, the plant residues decay is major mode of their production. Allelopathy occurs when the phenolic acids accumulate in the medium in relatively large amounts. The allelopathic potential of phenolic acids affects both the soil ecosystem and plant physiology (18,19,22,26). In soil, evidence shows that phenolic acids stimulates the soil dehydrogenase activity, soil microbial biomass carbon content and size of soil bacterial and fungal community (29). Additionally, experimental results have confirmed that plants residues rich in phenolic acids stimulates the invasion of soil-borne pathogens (12,14,21,28). Regarding plant physiology, concentration of phenolic acids and sensitivity of the recipient species are the key factors, determining the allelopathic activity of phenolic acids in plants. Generally phenolic acids are stimulatory to plants at very low concentrations, but inhibitory at high concentrations (15,20). The phenolic acids changes the plant physiology in many ways viz., gene expression, enzyme activity, membrane permeability, photosynthesis, protein and nucleic acid synthesis, etc. (2,4,8,9,24,27).

[*]Correspondence author; [1]Ningxia Key Laboratory of Microbial Resources Development and Applications in Special Environment, Yinchuan 750021, China.

Watermelon (*Citrullus lanatus* Thunb) is major cash crop worldwide and the China, ranks first in the world in its area (> 1.5 million hm^2). However, the rotation of watermelon is becoming more and more difficult due to the unknown factors leading to the development of soil sickness, which reduces its yield and quality. Extracts from roots, leaves or stems of various plants rich in phenolic acids, significantly inhibited the germination, seedling growth and radicle elongation (3,13,19,28); hence, phenolic acids are considered to play an important part in continuous cropping problem. To better understand the effects of phenolic acids on watermelon, the dose-effect relationship of individual compounds to watermelon need to be explored. The quantitative structure-activity relationship (QSAR) technique, which is already used in the field of biological activity evaluation and molecular design (7,10), may be used to explore the structure-antioxidant activity relationships of phenolic compounds (1,6). However, the structure-allelopathic activity relationship for phenolic compounds is still unknown. The 3D-QSAR of comparative molecular field analysis (CoMFA) and comparative molecular similarity index analysis (CoMSIA) can provide a 3D view to investigate the structural parts of phenolic compounds responsible for their inhibitory activity. Hence, the watermelon germination bioassay was done to determine the harmful biological effects of 21- phenolic acids, and their dose-effect relationships on watermelon seeds germination. The respective contribution of each key substituent to the allelopathy of phenolic acids was elucidated by the molecular field information in the 3D-QSAR (CoMFA & CoMSIA) models. This study aimed to elucidate the effects of phenolic acids on watermelon seed germination, and to provide a feasible method to evaluate the allelopathic and environmental risks of phenolic acid analogues.

METHODS AND MATERIALS

Chemicals

Information regarding the 21- test phenolic acids is given in Table 1. All compounds were purchased from Aladdin Company (Shanghai, China) and were of reagent grade (purity > 97%). Stock solutions of phenolic acids were prepared and diluted with double distilled water.

Seed Germination

Seeds of watermelon (*Citrullus lanatus* Thunb) were purchased from a seed supplier shop. The seeds were soaked for 10 min in sterile water at 60 ^oC and then for 6 h at 25 ^oC. Ten cm dia plastic Petri dishes with double layers of filter papers (Whatman filter paper No. 1) were sterilized at 121 ^oC for 20 min. Five sterilized seeds were sown per Petri dish and either 7 mL sterile water (blank control) or phenolic compound solution (concentration 0 to 200 µg/mL) was added per petri dish as per treatments on the 1st day and 2 mL on the 5th day. Petri dishes were kept in constant-temperature incubator, with 28±0.2 ^oC in dark. The germination (%) was recorded on the 3rd day after sowing and the radicle and hypocotyl length were measured on the 7th day with scale. The experiments of dose-response relationship of each phenolic acid were repeated thrice and the average IC_{50} (half-maximal inhibitory concentration) was calculated.

The half maximal inhibitory concentration (IC_{50}) were calculated in 3- ways: (i) $IC_{50,\ germination}$ was calculated using inhibition of germination induced by phenolic acids, (ii) $IC_{50,\ radicle}$ was calculated using inhibition of radicle length induced by phenolic acids, and (iii) $IC_{50,\ hypocotyl}$ was calculated using inhibition of hypocotyl length induced by phenolic acids.

Table 1. The experimental and model predicted values of allelopathic effects of phenolic acids on watermelon

No.	Names	CAS	IC_{50} (μg/mL)			$IC_{50,radicle}$ of QSARs（μmol/L）		
			$IC_{50,germination}$	$IC_{50,radicle}$	$IC_{50,hypocotyl}$	Exp.	CoMFA Pred.	CoMSIA II Pred.
1	Benzoic acid(BA）	65-85-0	98.34±5.74	67.86±5.24	78.68±7.14	555.69	593.289	562.948
2	Salicylic acid	69-72-7	122.92±5.86	73.68±7.55	59.36±8.21	533.45	576.147	571.381
3	4-HydroxyBA	99-96-7	93.97±6.17	79.26±7.37	72.68±5.56	573.87	575.577	563.59
4	Vanillic acid	121-34-6	99.86±8.59	86.31±6.13	59.26±4.21	513.25	526.573	547.303
5	2,5-DihydroxyBA	490-79-9	118.71±9.16	89.46±7.18	69.38±4.66	580.48	557.969	572.376
6	3,4-DihydroxyBA	99-50-3	139.26±12.92	98.45±3.97	64.49±6.71	638.78	575.568	596.233
7	Syringic acid	530-57-4	108.45±9.51	93.68±11.89	61.05±8.88	472.74	502.655	529.112
8	Cinnamic acid(CA）	140-10-3	103.71±11.07	77.19±5.33	73.73±4.81	521.01	518.147	486.565
9	*p*-Coumaric acid	501-98-4	126.89±8.59	76.91±5.86	64.57±5.47	468.48	500.842	486.983
10	3-HydroxyCA	14755-02-3	106.54±7.60	97.91±8.86	99.28±11.36	596.42	517.447	519.312
11	Caffeic acid	331-39-5	87.74±8.77	68.33±7.32	86.19±5.03	379.26	378.012	382.45
12	2,4-DihydroxyCA	614-86-8	122.22±8.91	84.88±7.81	76.33±6.18	471.11	480.926	492.447
13	Ferulic acid	1135-24-6	116.54±6.22	82.41±5.82	79.64±4.77	424.42	403.812	401.684
14	Isoferulic acid	537-73-5	98.01±5.09	71.89±4.90	90.87±3.71	370.21	409.677	415.642
15	3-MethoxyCA	6099-04-3	115.06±4.08	85.34±5.31	63.73±4.10	478.95	469.957	470.386
16	4-MethylCA	1866-39-3	94.86±7.52	78.09±6.45	84.13±10.56	481.49	486.963	484.08
17	2,3,4-TrimethoxyCA	33130-03-9	105.69±8.72	83.49±7.65	76.21±8.06	350.48	346.143	367.769
18	2-MethoxyCA	6099-03-2	104.01±4.54	85.56±6.77	83.29±4.91	480.21	488.74	476.649
19	3,5-DimethoxyCA	16909-11-8	123.09±8.07	96.88±8.59	77.78±6.54	465.29	397.472	382.211
20	2,3-DimethoxyCA	7345-82-6	101.38±7.60	83.37±6.54	108.91±8.59	400.41	401.753	394.805
21	Sinapic acid	530-59-6	112.86±8.81	78.96±6.98	106.94±9.83	331.44	379.771	383.514

QSAR method

Software SYBYL 8.0 (Tripos Inc., USA) was used to perform all the QSAR analyses. The 3D structures of all compounds were assessed using the standard tools; the main steps were: partial atomic charges were done by the Gasteiger-Huckel method, energy minimizations were conducted by the Tripos force field (energy gradient convergence criterion was 0.005 kcal/Å). The compound sinapic acid, with high inhibitory activity and most substituents on the benzene ring, was used as a template. Using the database alignment method, the other molecules were aligned to the template. The 3D view of aligned molecules is shown in Fig. 1.

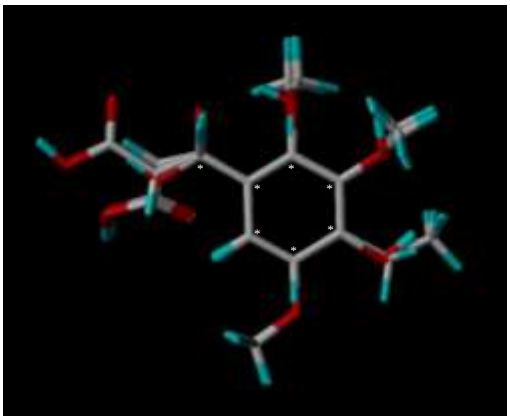

Figure 1. 3D-view of aligned molecules based on sinapic acid.
Note：atoms marked with * were selected for alignment of all structures.

For the CoMFA (comparative molecular field analysis) calculation, the molecules were placed into a 3D cubic lattice with 2 Å grid. A sp^3 carbon probe atom with +1 charge was used to calculate the interaction energies. The cutoff value for both steric and electrostatic fields was set to 30 kcal/mol. The CoMSIA (comparative molecular similarity index analysis) model was constructed by the same alignment used in CoMFA. Five fields of steric, electrostatic, hydrophobic, H-bond donor, and H-bond acceptor were generated using the standard settings.

In the CoMFA/CoMSIA modeling, $IC_{50,\ radicle}$ (μmol/L) values were used as dependent variables, and CoMFA/CoMSIA descriptors were used as the independent variables. Partial least square (*PLS*) regression was used for the statistical analysis. The leave-one-out (*LOO*) cross-validation was performed; the optimum number of components (*N*) and cross-validated correlation coefficient (Q^2) were obtained. Then, non-cross-validation analysis was conducted to yield the conventional multiple correlation coefficient (R^2), the standard error of estimate (*SEE*) and the Fisher test (*F*) values.

RESULTS

Dose-effect relationships

Twenty one phenolic acids were selected and tested based on two parameters: (i). compounds frequently detected in plant rhizospheres and (ii). compounds with typical structure suitable for QSAR modeling. The results were shown in Table 1. All the tested compounds suppressed the watermelon seeds germination at high concentrations,

$IC_{50,\ germination}$, $IC_{50,\ radicle}$ and $IC_{50,\ hypocotyl}$ from 87.74-139.26, 67.86-98.45 and 59.26-108.91 µg/mL, respectively. Growth indices of radicle and hypocotyl were more sensitive to phenolic acids inhibition than seeds germination. Statistical analysis showed that $IC_{50,\ germination}$ and $IC_{50,\ radicle}$ were positively correlated at 0.05 level, with Pearson correlation coefficient of 0.50; in contrast, $IC_{50,\ hypocotyl}$ was not correlated with the above two indicators.

Due to the structural diversity of phenolic acids, the inhibitory activities of these allelopathic compounds on germination were expected to be different. However, what kind of substituent and which substitution position contributed more to the inhibitory activity was unclear. Hence, the 3D-QSAR (by CoMFA and CoMSIA analyses) models were constructed to obtain more comprehensive and precise information.

3D-QSAR analysis

CoMFA and CoMSIA statistical results

The statistical results of the 3D-QSAR models were summarized in Table 2. For the CoMFA model, *LOO* analysis gave a cross-validated Q^2 value of 0.619 for three optimal components. The correlation coefficient R^2 was determined to be 0.819 for the non-cross validated *PLS* (partial least squares) analysis, *SEE* was 38.598 and *F* value was 25.657. The correlation between the experimental and predicted values were shown in Fig. 2(a). These indices suggested that a reliable CoMFA model was constructed successfully.

For the CoMSIA models, the statistical results of CoMSIA I revealed that the electrostatic, H-bond donor, H-bond acceptor and hydrophobic fields made the major contribution, whereas, the steric fields made a much smaller contribution. Hence, the CoMSIA II was constructed, in which the steric field was excluded. For the CoMSIA II model, a cross-validated Q^2 value of 0.645 was obtained with two optimal components, together with an R^2 value of 0.797, *SEE* value of 39.699 and *F* value of 35.475. The relationship between the experimental and predicted values (Fig. 2b) revealed that a better statistical correlation was achieved with the COMSIA II in comparison to the CoMSIA I model.

Interpretation of CoMFA contour maps

The CoMFA contour maps were depicted in Fig. 3. In the steric fields, green and yellow colours represented contours that were, sterically favorable and unfavorable to inhibitory activity, respectively. Hence, the green contours near R1, R2, R3 and R4 of the benzene ring indicated that substituents with big volume could increase the inhibitory activity of the molecules. The structure-activity relationship of substituents at R1/2/3/4 of phenolic acids were depicted in Table 3. For the R1 substituents, this finding was clearly supported by the higher activities of cinnamic acid derivatives with $-C_2H_2COOH$ substituent at the R1 position, whereas, the benzoic acid derivatives had -COOH at this site. For the substituents at R2/3/4, compounds with -OH or $-OCH_3$ groups at those sites exhibited higher inhibitory activity than unsubstituted compounds.

In the electrostatic fields, contours in blue and red represented positive charge groups favourable and unfavourable, respectively, to inhibitory activity. A small red contour near the area connecting R1 of the benzene ring indicated that greater electron density in this region was favourable, which was clearly supported by the higher inhibitory activity of cinnamic acid derivatives carrying the acrylic group at the substituent compared with benzoic acid derivatives that had the carboxyl group.

Table 2. Partial least squares (PLS) results

Index	Q^2	R^2	*SEE*	*F*	*N*	Contribution (%)				
						Steric	Electrostatic	Hydrophobic	Donor	Acceptor
CoMFA	0.619	0.819	38.598	25.657	3	50.3	49.7			
CoMSIA I	0.634	0.797	39.767	35.264	2	5.5	37.7	13.6	24.2	19.0
CoMSIA II	0.645	0.797	39.699	35.475	2		39.4	14.4	26.1	20.1

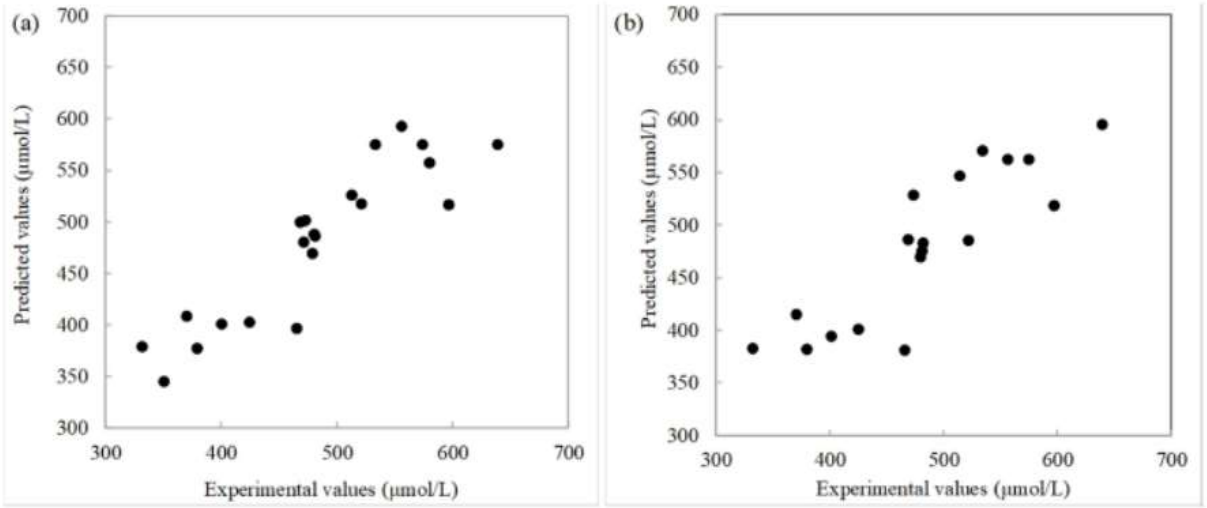

Figure 2. The relation schema of biological toxicity experimental values and predicted values. (a) CoMFA, (b) CoMSIAII

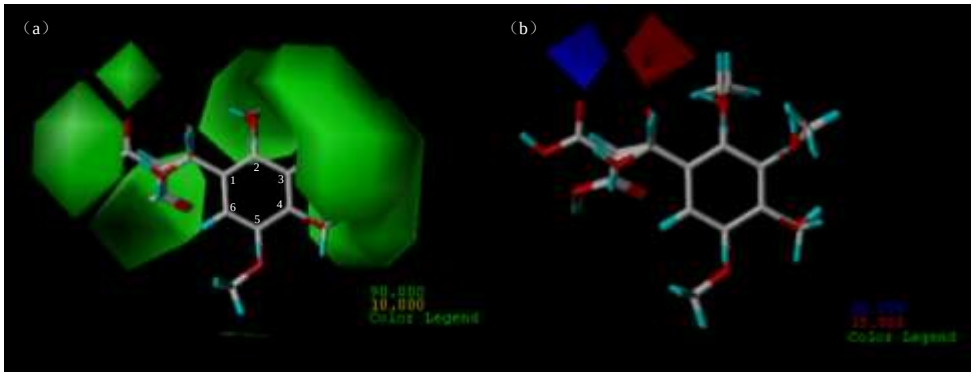

Figure 3. Contour maps of CoMFA model，(a) steric fields, (b) electrostatic fields.

Table 3. The structure-activity relationship of substituents at C-1/2/3/4 positon of phenolic acids

No.	Name	Structure	IC_{50} (μmol/L)	Name	Structure	IC_{50} (μmol/L)
	(a) The structure-activity relationship of substituents at C-1 positon of phenolic acids					
1	Benzoic acid(BA)		555.69	Cinnamic acid(CA)	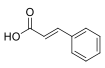	521.01
2	4-Hydroxy BA	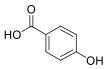	573.87	*p*-Coumaric acid	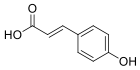	468.48
3	3,4-Dihydroxy BA	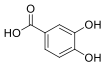	638.78	Caffeic acid	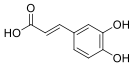	379.26
4	Vanillic acid	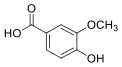	513.25	Ferulic acid	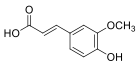	424.42
5	Syringic acid	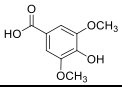	472.74	Sinapic acid	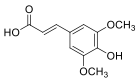	331.44
	(b) The structure-activity relationship of substituents at C-2 positon of phenolic acids					
1	Benzoic acid		555.69	Salicylic acid		533.45
2	Cinnamic acid	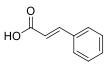	521.01	2-MethoxyCA	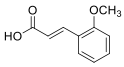	480.21
3	*p*-Coumaric acid	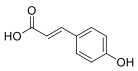	468.48	2,4-DihydroxyCA	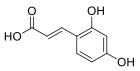	471.11
4	3-MethoxyCA	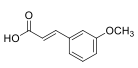	478.95	2,3-DimethoxyCA	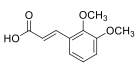	400.41

(c) The structure-activity relationship of substituents at C-3 positon of phenolic acids						
1	4-HydroxyBA	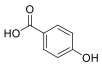	573.87	Vanillic acid	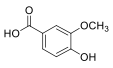	513.25
2	Cinnamic acid	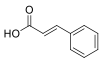	521.01	3-MethoxyCA	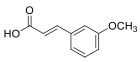	478.95
3	*p*-Coumaric acid	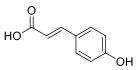	468.48	Ferulic acid	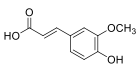	424.42
4	2-MethoxyCA	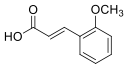	480.21	2,3-Dimethoxy CA	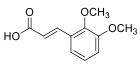	400.41
(d) The structure-activity relationship of substituents at C-4 positon of phenolic acids						
1	Benzoic acid		555.69	4-Hydroxy BA		573.87
2	Cinnamic acid	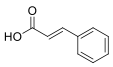	521.01	*p*-Coumaric acid	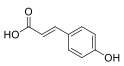	468.48
3	3-HydroxyCA	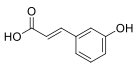	596.42	Caffeic acid	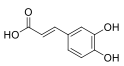	379.26
4	3,5-DimethoxyCA	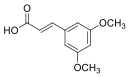	465.29	Sinapic acid	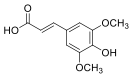	331.44

Interpretation of CoMSIA contour maps

(i). Electrostatic fields of CoMSIA II: These shown in Fig. 4(a), were generally in accordance with the electrostatic field distribution of CoMFA. However, an additional red contour was obtained in the region surrounding the R3 substituent, indicating that substituents with more negative charge at this site could be associated with increased inhibitory activity. This finding was well supported by the high inhibitory activities of vanillic acid, 3-methoxyCA, ferulic acid and 2,3-dimethoxyCA that carry the methyl group at the R3 substituent, whereas, the remaining compounds were unsubstituted.

(ii). Hydrophobic fields of CoMSIA II: These were depicted in Fig. 4(b). Contours in yellow and white represented regions where, hydrophobic and hydrophilic substituents were favorable to inhibitory activity respectively. A big yellow contour near the R3 and R4 substituents indicated that hydrophobic substituents at these two sites were favourable for inhibitory activity. This finding corresponded to the steric map provided by the CoMFA model, whereby the groups with big volume at the R3 and R4 led to strong inhibitory activity. The agreement of the CoMSIA II contour with that of CoMFA demonstrated suitability of the constructed models.

(iii). H-bond donor and acceptor fields of CoMSIA II: The H-bond donor fields of CoMSIA II were depicted in Fig. 4(c). The contours in cyan and purple represented the hydrogen bond donor groups favourable and unfavourable to inhibitory activity,

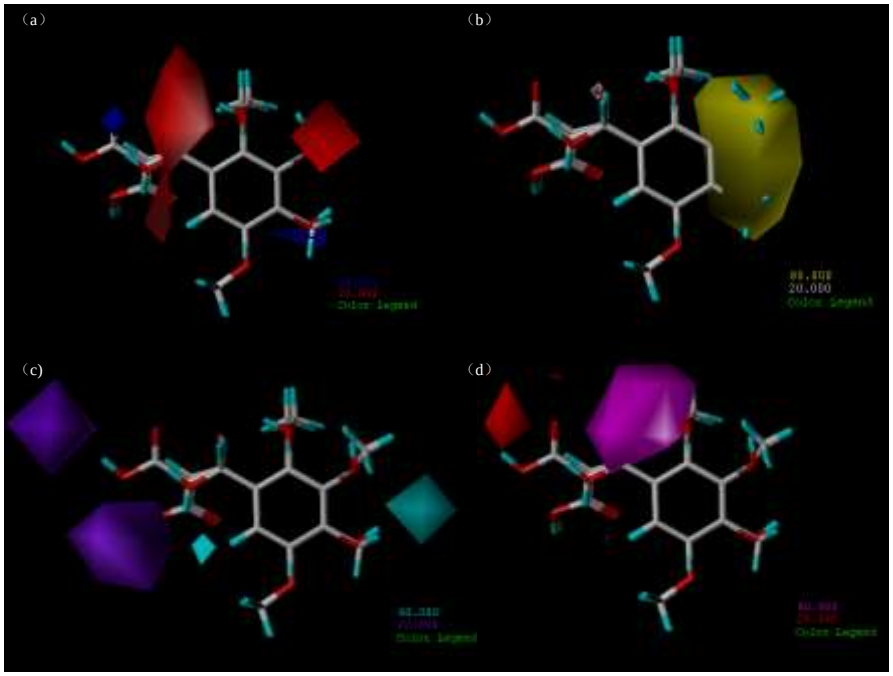

Figure 4. Contour maps of CoMSIA II model, (a) Electrostatic fields, (b) Hydrophobic fields, (c) H-bond donor fields, (d) H-bond acceptor fields

respectively. Two big purple contours appeared in the R1 region, indicating that the H-bond donors derived from carboxyl groups decreased the inhibitory activity. A small cyan-colored contour near the R4 substituent indicated that substituents with H-bond donor characteristic at R4 increased the inhibitory activity. This argument was further supported by the high activity of *p*-coumaric acid, caffeic acid and sinapic acid with hydroxyl group at R4, whereas, the rest of compounds were unsubstituted. The H-bond acceptor fields of CoMSIA II were depicted in Fig. 4(d). The contours in magenta and red represented the hydrogen-bond acceptor groups favourable and unfavourable to inhibitory activity, respectively. A big magenta near the R2 substituent indicated the location of H-bond acceptor groups increased the inhibitory activity. For instance, compounds 2-methoxyCA and 2,3-dimethoxyCA with the methoxyl substituent at R2, as a typical hydrogen-bond acceptor group, increased the inhibitory activity than unsubstituted compounds.

DISCUSSION

Long-term monoculture of watermelon leads to the growth inhibition, decreases the crop yields and quality due to development of soil sickness (12,25), and allelopathy is one of the important contributing factors. Although a variety of phenolic acids co-exist in the rhizosphere of watermelon, how many are present and how toxic each compounds are the keys to their allelopathic action. Germination is very sensitive phase in plant growth cycle. Investigating the suppression of watermelon seeds germination by exogenous phenolic acids is of great significance. The dose-effect relationship suggested that phenolic acids decreased the seeds germination of watermelon at 59.26-139.26

μg/mL. However, the concentration of phenolic acids in the rhizosphere soil around plant roots was significantly lower than inhibitory concentrations obtained under laboratory conditions (4). Hence, it is reasonable to infer that single phenolic acid could not lead to allelopathic inhibition of watermelon.

By sharing the common benzene ring and active carboxylic group, various substituent types and positions on the ring contributed to the structural diversity and allelopathic activities of phenolic acids. In general, the contour maps of the CoMFA and CoMSIA models can be used to explore the toxicity mechanisms of the compounds of interest (11,23). In the CoMFA model, the steric fields contributed 50.3 % of inhibition, indicating that non-specific reactions accounted for a large proportion of the inhibitory action. In both the CoMFA and CoMISA II models, the electrostatic fields made a major contribution as well, which suggested that electron transfer might have existed between the phenolic acids and watermelon seeds.

CONCLUSIONS

The allelopathic activity of 21 phenolic compounds was studied based on watermelon seeds germination assay and 3D-QSAR modeling. The results suggested that the inhibitory effects of each individual compound to watermelon seeds germination were weak, with the IC_{50} values in the ~μg/mL range. The 3D-QSAR was done using the CoMFA and CoMSIA tools, The Q^2 values of CoMFA (Q^2 = 0.619, R^2 = 0. 819) and CoMSIA II (Q^2 = 0.645, R^2 = 0.797) indicated the statistical validity (Q^2 > 0.5). The QSAR results suggested that the compounds with bigger moieties and/or negative charge at R1, with bigger moieties and/or H-bond acceptor at R2, with bigger moieties and/or negative charge at R3, and bigger moieties and/or H-bond donor at R4 increased the inhibition of watermelon seeds germination.

ACKNOWLEDGEMENTS

This work was financially supported by the Natural Science Foundation of Ningxia Province, China (No. 2020AAC03256), as well as the project of State Key Laboratory of Environmental Chemistry and Ecotoxicology, Research Center for Eco-Environmental Sciences, Chinese Academy of Sciences (No. KF 2018-07). We are grateful to Dr. DongBin Wei from the Research Center for Eco-Environmental Sciences, Chinese Academy of Sciences, for his help in QASR modeling.

REFERENCES

1. Amić, A., Marković, Z., Dimitrić Marković, J. M., Stepanić, V., Lučlć, B. and Amić, D. (2014). Towards an improved prediction of the free radical scavenging potency of flavonoids: The significance of double PCET mechanisms. *Food Chemistry* **15:** 578-585.
2. Baziramakenga, R., Leroux, G. D. and Simard, R. R. (1995). Effects of benzoic acid on membrane permeability of soybean roots. *Journal of Chemical Ecology* **21:** 1271-1285.
3. Bi, Y. M., Jiao, X. L., Li, X. X., Tian, G. L., Li, L., Liu, H. L. and Gao, W. W. (2020). Degradation dynamics of nine phenolic acids in American ginseng and maize grown soils. *Allelopathy Journal* **49:** 73-87.
4. Blum, U. and Gerig, T. M. (2005). Relationships between phenolic acid concentrations, transpiration, water utilization, leaf area expansion and uptake of phenolic acids: Nutrient culture studies. *Journal of Chemical Ecology* **31:** 1907-1932.
5. Blum, U., Wentworth, T. R., Klein, K., Worsham, A. D., King, L. D., Gerig, T. M. and Lyu, S. W. (1991). Phenolic acid content of soils from wheat-no till, wheat-conventional till, and fallow-conventional till soybean cropping systems. *Journal of Chemical Ecology* **17:** 1045-1068.

6. Chen, Y., Xiao, H., Zheng, J. and Liang, Z. (2015). Structure-thermodynamics-antioxidant activity relationships of selected natural phenolic acids and derivatives: An experimental and theoretical evaluation. *Plos One* **10:** e0121276.
7. Cherkasov, A., Muratov, E. N., Fourches, D., Varnek, A., Baskin, I., Cronin, M., Dearden, J., Gramatica, P., Martin, Y. C., Todeschini, R., Consonni, V., Kuzmin, Vi. E., Cramer, R., Benigni, R., Yang, C., Rathman, J., Terfloth, L., Gasteiger, J., Richard, A. and Tropsha, A. (2014). QSAR modeling: Where have you been? Where are you going to? *Journal of Medicinal Chemistry* **57:** 4977-5010.
8. Chi, W. C., Chen, Y. A., Hsiung, Y. C., Fu, S. F., Chou, C. H., Trinh, N. N., Chen, Y. C. and Huang, H. J. (2013). Autotoxicity mechanism of *Oryza sativa*: Transcriptome response in rice roots exposed to ferulic acid. *BMC Genomics* **14:** 1-18.
9. Coelho, E. M. P., Barbosa, M. C., Mito, M. S., Mantovanelli, G. C., Oliveira Jr, R. S. and Ishii-Iwamotoet, E. L. (2017). The activity of the antioxidant defense system of the weed species *Senna obtusifolia L.* and its resistance to allelochemical stress. *Journal of Chemical Ecology* **43:** 1-14.
10. Cumming, J.G., Davis, A.M., Muresan, S., Haeberlein, M. and Chen, H.M. (2013). Chemical predictive modelling to improve compound quality. *Nature Reviews Drug Discovery* **12:** 948-962.
11. Fan, D., Liu, J., Wang, L, Yang, X.H., Zhang, S.H., Zhang, Y. and Shi, L. (2016). Development of quantitative structure–activity relationship models for predicting chronic toxicity of substituted benzenes to *Daphnia magna*. *Bulletin of Environmental Contamination and Toxicology* **96:** 664-670.
12. Hao, W.Y., Ren, L.X., Ran, W. and Shen, Q.R. (2010). Allelopathic effects of root exudates from watermelon and rice plants on *Fusarium oxysporum* f. sp. *Niveum*. *Plant and Soil* **336:** 485-497.
13. Hao, Z.P., Wang, Q., Christie, P. and Li, X.L. (2007). Allelopathic potential of watermelon tissues and root exudates. *Scientia Horticulturae* **112:** 315-320.
14. Hartung, A.C. and Stephens, C.T. (1983). Effects of allelopathic substances produced by asparagus on incidence and severity of asparagus decline due to *Fusarium* crown rot. *Journal of Chemical Ecology* **9:** 1163-1174.
15. Hozawa, M. and Nawata, E. (2020). Allelopathic effects of leaf litter leachates of *Ulex europaeus* on other species and its own seed germination. *Allelopathy Journal* **49:** 217-228.
16. Jayasena, T., Poljak, A., Smythe, G., Braidy, N., Münch, G. and Sachdev, P. (2013). The role of polyphenols in the modulation of sirtuins and other pathways involved in Alzheimer's disease. *Ageing Research Reviews* **12:** 867-883.
17. Jiang, G.Y., Li, Y.B. and Liu, J.G. (2013). Autotoxicity potential of cotton tissues and root exudates and identification of its autotoxins. *Allelopathy Journal* **32:** 279-288.
18. Jin, X., Shi, Y.J., Tan, S.C., Ma, C.L., Wu, F.Z., Pan, K. and Zhou, X.G. (2019). Effects of cucumber root exudates components on soil bacterial community structure and abundance. *Allelopathy Journal* **48:** 167-174.
19. Lara-Núñez, A., Sánchez-Nieto, S., Anaya, A. L. and Cruz-Ortega, R. (2010). Phytotoxic effects of *Sicyos deppei* (*Cucurbitaceae*) in germinating tomato seeds. *Physiologia Plantarum* **136:** 180-192.
20. Li, Q., Zhang, L.X., Guan, T.Z., Xu, Y.H. and Chen, C.B. (2020). Allelopathic effects of ginsenoside Rgl on seed germination and seedling growth of *Panax ginseng*. *Allelopathy Journal* **49:** 229-242.
21. Peirce, L.C. and Miller, H.G. (1993). Asparagus emergence in *fusarium*-treated and sterile media following exposure of seeds or radicles to one or more cinnamic acids. *Journal of the American Society for Horticultural Science* **118:** 23-28.
22. Rugare, J.T., Pieterse, P.J. and Mabasa, S. (2020). Effects of green manure cover crops (*Canavali aensiformis L.* and *Mucuna pruriens L.*) on seed germination and seedlings growth of maize and *Eleusine indica L.* and *Bidens pilosa L.* weeds. *Allelopathy Journal* **50:** 121-139.
23. Salahinejad, M. and Ghasemi, J.B. (2014). 3D-QSAR studies on the toxicity of substituted benzenes to *Tetrahymena pyriformis*: CoMFA, CoMSIA and VolSurf approaches. *Ecotoxicology and Environmental Safety* **105:** 128-134.
24. Santos, W.D.D., Ferrarese, M.L.L., Nakamura, C.V., Mourão, K.S.M., Mangolin, C.A. and Ferrarese-Filho, O. (2008). Soybean (*Glycine max*) root lignification induced by ferulic acid. The possible mode of action. *Journal of Chemical Ecology* **34:** 1230-41.
25. Song, Y., Kong, Y., Wang, J., Ruan, Y, Huang, Q.W., Ling, N. and Chen Q.R. (2018). Identification of the produced volatile organic compounds and the involved soil bacteria during decomposition of watermelon plant residues in a *Fusarium*-infested soil. *Geoderma* **315:** 178-187.
26. Wang, R L., Liu, S.W., Xin, X.W., Chen, S., Peng, G.X., Su, Y.J. and Song, Z.K. (2017). Phenolic acids contents and allelopathic potential of 10-cultivars of alfalfa and their bioactivity. *Allelopathy Journal* **40:** 63-70.
27. Wu, B., Long, Q., Gao, Y., Wang, Z., Shao, T.W., Liu, Y.N., Li, Y. and Ding, W.L. (2015). Comprehensive characterization of a time-course transcriptional response induced by autotoxins in *Panax ginseng* using RNA-Seq. *BMC Genomics* **16:** 1010-1025.
28. Yu, J.Q., Shou, Y., Qian, R., Hu, W.H., Yu, J. Q., Shou, S.Y., Qian, Y.R. and Hu, W.H. (2000). Autotoxic potential of cucurbit crops. *Plant and Soil* **223:** 147-151.
29. Zhou, X. and Wu, F. (2013). Artificially applied vanillic acid changed the soil microbial communities in the rhizosphere of cucumber (*Cucumis sativus L.*). *Canadian Journal of Soil Science* **93:** 13-21.